

Highly Efficient Year-Round Energy and Comfort Optimization of HVAC Systems in Electric City Buses^{*}

Fabio Widmer^{*} Andreas Ritter^{*} Mathias Achermann^{*}
Fabian Büeler^{*} Joshua Bagajo^{*} Christopher H. Onder^{*}

^{*} *Institute for Dynamic Systems and Control, ETH Zürich, 8092
Zürich, Switzerland (e-mail: fawidmer@idsc.mavt.ethz.ch)*

Abstract: In this paper, we present a novel approach to perform highly efficient numerical simulations of the heating, ventilation, and air-conditioning (HVAC) system of an electric city bus. The models for this simulation are based on a steady-state assumption. We show two solution approaches to obtain the minimum energy requirement for a certain thermal comfort criterion subject to specific ambient conditions. Thanks to the computationally efficient approach, we can evaluate the model on a large dataset of 7500 scenarios in various ambient conditions to estimate the year-round performance of the system subject to different comfort requirements. Thereby, we can show that a heat pump (HP) can reduce the annual mean power consumption by up to 60%, compared to a heating strategy based on positive temperature coefficient (PTC) elements. Ceiling-mounted radiant heating elements complementing a PTC heating system can reduce the annual mean power consumption by up to 10%, while they cannot improve the energy efficiency when used in conjunction with a HP. Finally, a broad sensitivity study reveals the fact that improving the HP's coefficient of performance (COP) has the largest leverage in terms of mean annual power consumption. Moreover, improving the COP of the cooling mode yields significantly lower benefits, as the annual energy expenditure for heating is around eight times larger than for cooling.

Keywords: HVAC, model-based optimization, thermal comfort, electrified public transport, design sensitivities, Pareto optimality, radiant heating

1. INTRODUCTION

1.1 Motivation

Global warming currently is one of the greatest challenges faced by humanity. One of the necessary steps to overcome this challenge is to phase out the use of fossil fuels. This urge is reinforced by the current global energy crisis, initially caused by the COVID-19 pandemic and further fueled in Europe by the military conflict between Russia and Ukraine. These effects are leading to a massive increase of battery electric vehicle (BEV) sales all around the world according to Bibra et al. (2022).

However, although BEVs offer clear advantages with regard to their propulsion efficiency, the comparably high demand of energy for the HVAC system is still an open issue. On the one hand, the HVAC consumption is more relevant for BEVs compared to combustion-based vehicles since waste heat from traction components is not abundantly available. On the other hand, the high HVAC consumption directly influences the achievable driving range, which is generally one of the sensitive topics with regards to BEVs. For urban public transport vehicles these effects are even

more pronounced due to the poor insulation of the passenger cabin and the frequent door openings. For instance, Cigarini et al. (2021) show that in winter conditions the HVAC energy consumption of an electric city bus can be almost half the overall energy consumption.

Therefore, analyzing and optimizing the HVAC systems is a very active topic in research and industry, not only in public transport but for all types of vehicles. For instance, various suppliers have joined forces to put together a prototype electric bus with a HP, seat heaters and phase change material (PCM) heating elements, as reported by Hanke (2018), thus demonstrating the applicability of these concepts in practice. Additionally, the use of radiant heater (RH) panels or alternative refrigerants like CO₂ (R744) are investigated for passenger vehicles by Qi (2014) and Cvok et al. (2021), respectively. Evaluating and comparing the performance of such concepts requires a method to efficiently calculate the achievable trade-off between the energy consumption and the thermal comfort of a given HVAC concept on a set of scenarios that represent a typical year-round operation.

1.2 Literature

In the scientific context, such evaluations typically are based on numerical simulations, which allow much quicker evaluation of changes in HVAC concepts compared to

^{*} **This work has been submitted to IFAC for possible publication.** It has been supported by the Swiss Federal Office of Energy (SFOE, contract number SI/501979-01) and the industrial partners Carrosserie HESS AG and Verkehrsbetriebe Zürich (VBZ).

physical experiments. Thereby, most of the work presented in the literature relies on dynamic models, which allow simulations of transient processes, e.g., the initial cabin conditioning (heat-up or cool-down) as studied by Ramsey et al. (2022). Such transient processes are particularly relevant for passenger vehicles, where the typical trip length is not significantly longer than this transient phase. Also, dynamic models are needed to analyze or compare control approaches, as presented e.g. by Schaut and Sawodny (2020). However, as these dynamic simulations are numerically expensive, typically only single scenarios are considered, the results of which might not be representative for the year-round operation of a vehicle.

1.3 Research Statement

In contrast to the above-mentioned dynamic models suitable for the simulation of passenger vehicles, we suggest the use of steady-state models for the analysis of HVAC systems in urban public transport vehicles such as city buses. The rationale for this proposal is a clear separation of timescales between the relevant dynamics, which are in the order of tens of minutes, and the disturbances, which have time constants of the order of tens of seconds (door openings, change of driving speed) or hours (ambient conditions like temperature). Throughout the period of one hour, the operation of the HVAC system of such vehicles can thus be considered to be in steady state. Clearly, these assumptions are not valid for many other thermal systems, such as passenger cars during heat-up conditions or buildings, the thermal dynamics of which are much slower and are thus in the same order of magnitude as those of ambient condition changes.

We therefore believe that a steady-state model along with an efficient evaluation algorithm can be a viable tool to analyze the HVAC systems of city buses. By neglecting all system dynamics, the evaluation of the trade-off between the power consumption and the thermal comfort for specific ambient conditions is much quicker, which allows to expose the system not only to a small selection of ambient conditions, but to a great number of scenarios representative of a year-round operation. To the best of our knowledge, such a holistic sensitivity analysis of the HVAC system of an electric city bus based on steady-state calculations has not yet been proposed in the literature.

1.4 Paper Structure

The remainder of this text is structured as follows: Section 2 introduces the mathematical models. Section 3 presents two solution approaches to determine the smallest power consumption of the system necessary to satisfy the thermal comfort requirements. Section 4 introduces the scenarios defining the ambient conditions of the case study, which are then used to generate the results shown in section 5. Finally, section 6 concludes this work and lists potential future research directions.

2. MODEL

Figure 1 provides a graphical overview of all model components. It shows the four thermal reservoirs with their

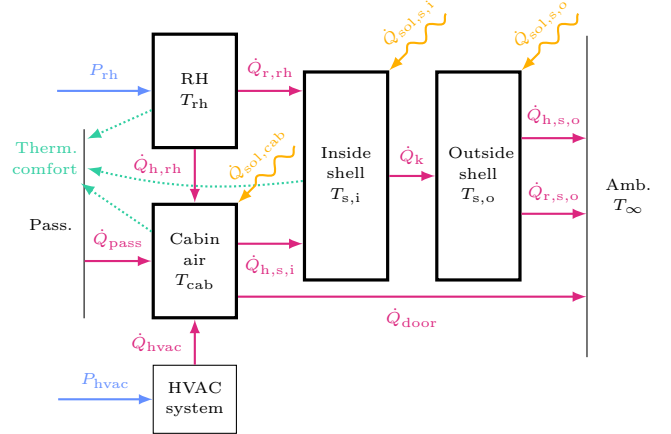


Fig. 1. Model overview including the thermal reservoirs (bold blocks) and the connecting flows. Red and yellow arrows denote heat flows, blue arrows denote electric power flows, and green dotted arrows denote the influence on thermal comfort.

respective temperature variables, i.e., the RH temperature T_{rh} , the cabin air temperature T_{cab} , and the inside and outside shell surface temperatures $T_{s,i}$ and $T_{s,o}$. The ambient is assumed to be at a uniform temperature T_{∞} .

In the following, we first introduce the models that describe all thermal and electric flows between these components. Second, we explain the models used to determine thermal comfort.

2.1 Heat Flows

Metabolic Heat: The heat emitted by passengers is described by

$$\dot{Q}_{pass} = N_{pass} \cdot \dot{Q}_{met}, \quad (1)$$

where N_{pass} represents the number of passengers in the bus and $\dot{Q}_{met} = 125 \text{ W}$ represents the metabolic heat rate of the human organism, for which we assume sedentary activity according to EN ISO 7730.

Convection: For the convective heat transfer, we use

$$\dot{Q}_{h,rh} = h_{rh} \cdot A_{rh} \cdot (T_{rh} - T_{cab}), \quad (2)$$

$$\dot{Q}_{h,s,i} = h_{s,i} \cdot A_{body} \cdot (T_{cab} - T_{s,i}), \quad (3)$$

$$\dot{Q}_{h,s,o} = h_{s,o} \cdot A_{body} \cdot (T_{s,o} - T_{\infty}), \quad (4)$$

for the surfaces of the RHs, and the inside and outside shell, respectively. The values for the convective heat transfer coefficients $h_{rh} = 2.1 \frac{\text{W}}{\text{m}^2\text{K}}$, $h_{s,i} = 8.0 \frac{\text{W}}{\text{m}^2\text{K}}$, and $h_{s,o} = 20.7 \frac{\text{W}}{\text{m}^2\text{K}}$ are based on EN ISO 6946 and adjusted for increased air movement inside the cabin and an average bus velocity of $15 \frac{\text{km}}{\text{h}}$. The surface area of the entire bus hull is represented by $A_{body} = 199 \text{ m}^2$. A_{rh} denotes the RH surface area, which is varied between simulations.

Conduction: For the conductive heat transfer through the shell, we use

$$\dot{Q}_k = k_{body} \cdot A_{body} \cdot (T_{s,i} - T_{s,o}), \quad (5)$$

with the mean heat conductance through the bus enclosure given by $k_{body} = 6.9 \frac{\text{W}}{\text{m}^2\text{K}}$. This value is calculated to

match an overall U-value of $2.9 \frac{\text{W}}{\text{m}^2\text{K}}$, which has been determined for a city bus in a climate chamber by Sidler et al. (2019). As this U-value is over ten times larger than the one of modern buildings, we expect very high heat losses through the shell of the bus.

Door Losses: To estimate the losses through open doors, we rely on the models developed by Schälin (1998), which are based on Bernoulli's law, the ideal gas law, and some simplifying assumptions. Accordingly, we derive the following equation for the heat loss through the doors with height $h_{\text{door}} = 1.95 \text{ m}$ and combined overall width $w_{\text{door,tot}} = 4.4 \text{ m}$:

$$\dot{Q}_{\text{door}} = \frac{\rho_{\infty} \cdot c_{p,a} \cdot C_d \cdot \sqrt{g \cdot h_{\text{door}}^3}}{3} \cdot \sqrt{\frac{T_{\text{cab}} - T_{\infty}}{T_{\infty}}} \cdot (T_{\text{cab}} - T_{\infty}) \cdot w_{\text{door,tot}} \cdot \zeta_{\text{door}}. \quad (6)$$

The variables $\rho_{\infty} = 1.25 \frac{\text{kg}}{\text{m}^3}$ and $c_{p,a} = 1005 \frac{\text{J}}{\text{kgK}}$ represent the air density and heat capacity, respectively, and $g = 9.81 \frac{\text{m}}{\text{s}^2}$ represents earth's gravitational constant. The discharge coefficient $C_d = 0.6$ is an empirical factor accounting for various sources of losses in the flow. The fraction $\zeta_{\text{door}} \in [0, 1]$ allows to specify the fraction of time the doors are open.

Solar Irradiation: We consider both direct and diffuse solar irradiation. Therefore, we use measured data of the direct normal irradiance (DNI) I_{dni} and the diffuse horizontal irradiance (DHI) I_{dhi} from a meteorological station from the Swiss Federal Office of Meteorology and Climatology (MeteoSwiss). Assuming a solar altitude angle β , a solar azimuth angle ϕ , isotropic diffuse radiation, and neglecting ground-reflected irradiance, the irradiance on the roof and the wall of the bus are given by

$$I_{\text{roof}} = \cos\left(\frac{\pi}{2} - \beta\right) \cdot I_{\text{dni}} + I_{\text{dhi}}, \quad (7)$$

$$I_{\text{wall}} = \cos\beta \cdot \max\{\cos(\phi - \psi), 0\} \cdot I_{\text{dni}} + \frac{1}{2} \cdot I_{\text{dhi}}, \quad (8)$$

respectively, where the surface azimuth ψ corresponds to the azimuth angle of the wall surface normal. Assuming the bus is driving in all directions with equal probability (i.e., averaging over ψ), the mean irradiance on the wall can be simplified to

$$\bar{I}_{\text{wall}} = \frac{\cos\beta}{\pi} \cdot I_{\text{dni}} + \frac{1}{2} \cdot I_{\text{dhi}}. \quad (9)$$

Hence, the total heat by solar irradiation incident on the outside shell of the cabin is given by

$$\dot{Q}_{\text{sol,s,o}} = (1 - \zeta_{\text{sh}}) \cdot \left(A_{\text{roof}} \cdot I_{\text{roof}} \cdot \alpha_{\text{paint}} \cdot (1 - \zeta_{\text{roof}}) + A_{\text{wall}} \cdot \bar{I}_{\text{wall}} \cdot (1 - \zeta_{\text{win}}) \cdot \alpha_{\text{paint}} \right), \quad (10)$$

where $A_{\text{roof}} = 48.6 \text{ m}^2$ and $A_{\text{wall}} = 102 \text{ m}^2$ represent the roof surface area and the combined surface area of all walls. For all surfaces, which are painted in bright colors, we use $\alpha_{\text{paint}} = 0.3$ based on data from Incropera et al. (2007). The fractions $\zeta_{\text{roof}} = 0.7$ and $\zeta_{\text{win}} = 0.35$ represent the fraction of the roof that is shaded by components (e.g., batteries), and the fraction of the walls that are windows, respectively. For the fraction ζ_{sh} representing the fraction of time where the bus is in the shade (e.g., by buildings or

bridges), we use season-dependent values for urban areas as suggested by Centeno Brito et al. (2021).

The solar radiation transmitted into the bus through the windows is assumed to be fully absorbed by the bus interior. A fraction $\zeta_{\text{cab}} = 0.5$ of this heat denoted $\dot{Q}_{\text{sol,cab}}$ is assumed to be absorbed directly by the cabin air, which allows to represent surfaces that are not directly connected to the shell, such as seats or passenger surfaces. The remainder of the incident irradiation, denoted $\dot{Q}_{\text{sol,s,i}}$, is absorbed by the inner shell:

$$\dot{Q}_{\text{sol,cab}} = (1 - \zeta_{\text{sh}}) \cdot A_{\text{wall}} \cdot \bar{I}_{\text{wall}} \cdot \zeta_{\text{win}} \cdot \tau_{\text{win}} \cdot \zeta_{\text{cab}}, \quad (11)$$

$$\dot{Q}_{\text{sol,s,i}} = (1 - \zeta_{\text{sh}}) \cdot A_{\text{wall}} \cdot \bar{I}_{\text{wall}} \cdot \zeta_{\text{win}} \cdot \tau_{\text{win}} \cdot (1 - \zeta_{\text{cab}}), \quad (12)$$

where the transmissivity of the windows to solar radiation is given by $\tau_{\text{win}} = 0.8$ based on Incropera et al. (2007).

Thermal Radiation: We assume all surfaces to be perfect emitters for simplicity, which does not introduce major errors at around room temperature according to Incropera et al. (2007). The windows are assumed opaque to this far-infrared radiation. Assuming a uniform ambient temperature, the heat incident on the outside of the bus is thus given by

$$\dot{Q}_{\text{r,s,o}} = \sigma \cdot A_{\text{body}} \cdot (T_{\text{s,o}}^4 - T_{\infty}^4), \quad (13)$$

where $\sigma = 5.67 \times 10^{-8} \frac{\text{W}}{\text{m}^2\text{K}^4}$ is the Stefan-Boltzmann constant. Assuming that all RH panels are mounted in a coplanar arrangement on the ceiling of the bus, their mutual view factor is zero and thus, the view factor from the infrared heaters to the inner bus shell is one. Thus, the net radiative heat transfer from the RHs to the inside shell becomes

$$\dot{Q}_{\text{r,rh}} = \sigma \cdot A_{\text{rh}} \cdot (T_{\text{rh}}^4 - T_{\text{s,i}}^2). \quad (14)$$

Controlled Heat Flows: The power necessary for heating of the RH panels is given by P_{rh} . We assume that this electric power is fully converted into heat and that the RH panels are insulated against the ceiling. The heat provided by the HVAC system is denoted \dot{Q}_{hvac} . Utilizing a vapor compression cycle (VCC) allowing air-conditioning (AC) and HP modes, the electric input power can be calculated by

$$P_{\text{hvac}} = \frac{|\dot{Q}_{\text{hvac}}|}{\gamma(T_{\text{cab}} - T_{\infty})}, \quad (15)$$

where $\gamma(T_{\text{cab}} - T_{\infty})$ represents the coefficient of performance (COP) for both heating and cooling, depending on the temperature difference between the two thermal reservoirs, as shown in the top left graph of fig. 2. This formulation also allows to consider purely resistive heating (e.g., based on PTC elements) by selecting a COP of one for heating scenarios.

Heat Balance: In our experience, the time constant of the relevant dynamics of the HVAC system of public transport vehicles is in the order of tens of minutes. On the other hand, the relevant disturbances either have time constants in the order of tens of seconds, as e.g. in the case of door openings and the driving profile, or hours, as e.g. in the case of ambient temperature. We thus conclude that for high-level energetic analyses, the operation of the HVAC system of a city bus can be approximated by the

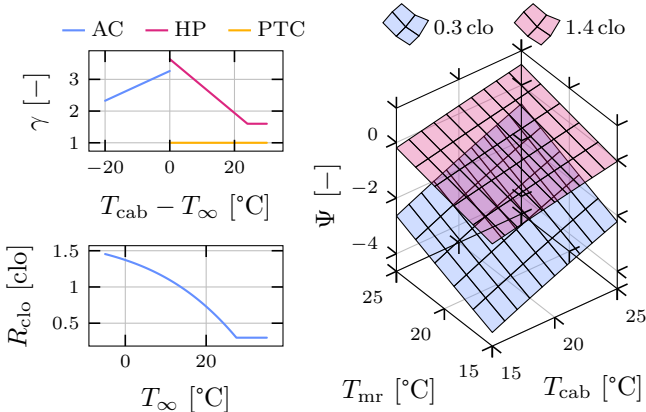


Fig. 2. Visualization of temperature-dependent models. The left graphs shows the COP of an R407c VCC and the clothing insulation. The right graph shows the predicted mean vote (PMV) for two different clothing values.

system's steady state. As a result, the following system of equations can be formulated for the heat balance:

$$0 = \begin{bmatrix} \dot{Q}_{\text{pass}} + \dot{Q}_{\text{h,rh}} - \dot{Q}_{\text{h,s,i}} - \dot{Q}_{\text{door}} + \dot{Q}_{\text{sol,cab}} + \dot{Q}_{\text{hvac}} \\ P_{\text{rh}} - \dot{Q}_{\text{r,rh}} - \dot{Q}_{\text{h,rh}} \\ \dot{Q}_{\text{r,rh}} + \dot{Q}_{\text{h,s,i}} + \dot{Q}_{\text{sol,s,i}} - \dot{Q}_{\text{k}} \\ \dot{Q}_{\text{k}} - \dot{Q}_{\text{h,s,o}} - \dot{Q}_{\text{r,s,o}} + \dot{Q}_{\text{sol,s,o}} \end{bmatrix}, \quad (16)$$

where the four equations correspond to the energy conservation equations of the corresponding thermal reservoirs.

2.2 Thermal Comfort

We model thermal comfort according to the model of Fanger (1970), which forms the basis of the norm EN ISO 7730. The model characterizes the thermal comfort in terms of the PMV, ranging from -3 (“cold”) to $+3$ (“hot”). For our calculations, we assume a constant air velocity of $v_{\text{cab}} = 0.1 \frac{\text{m}}{\text{s}}$ and a constant relative humidity of $\phi_{\text{cab}} = 40\%$. For the metabolic heat rate, we use 1.2 met , which is consistent with the assumption in eq. (1). Thus, the PMV can be calculated as a function of the variables air temperature T_{cab} , mean radiant temperature T_{mr} , and clothing insulation factor R_{clo} :

$$\Psi = f(T_{\text{cab}}, T_{\text{mr}}, R_{\text{clo}}(T_{\infty}), v_{\text{cab}}, \phi_{\text{cab}}, \dot{Q}_{\text{pass}}), \quad (17)$$

for which we show two sample visualizations in the right graph of fig. 2. The clothing insulation factor R_{clo} quantifies the clothing of the passengers, which depends on the ambient temperature as shown in the bottom left graph of fig. 2. The relationship we use for this purpose is based on a model presented by Havenith et al. (2012). We additionally introduce a lower limit of $R_{\text{clo}} = 0.3$ in summer since we do not expect passengers to be dressed lighter in accordance to EN ISO 7730. Furthermore, we assume that passengers do not change clothing when entering a city bus.

To determine the mean radiant temperature T_{mr} , we describe a passenger by an upright cuboid with dimensions $0.25 \text{ m} \times 0.25 \text{ m} \times 1.7 \text{ m}$, which does not take part in the radiation balance of the enclosure. The passenger can thus be considered a “passive” sensory device, apart from its metabolic heat release given in eq. (1). Using the view

factor relations given in Incropera et al. (2007), the mean radiant temperature of a passenger is given by

$$T_{\text{mr}}^4 = \frac{T_{\text{s,i}}^4 \cdot \sum_i (A_i \cdot F_{i \rightarrow \text{s,i}}) + T_{\text{rh}}^4 \cdot \sum_i (A_i \cdot F_{i \rightarrow \text{rh}})}{\sum_i A_i}, \quad (18)$$

where the index i is used to iterate over the five surfaces of the cuboid. The view factors necessary for this calculation can be determined analytically as shown by Gross et al. (1981). Finally, to obtain an overall estimate for the PMV, we average the passengers' PMVs calculated in eq. (17).

3. SOLUTION APPROACH

Within this work, our goal is to minimize the power demand

$$P_{\text{tot}} = P_{\text{rh}} + P_{\text{hvac}}, \quad (19)$$

while respecting a certain comfort interval

$$\Psi \in [\Psi_{\text{min}}, \Psi_{\text{max}}]. \quad (20)$$

By allowing the PMV to be in a certain comfort interval instead of prescribing a specific PMV target, we can evaluate the achievable trade-off between the power consumption and the comfort achieved as a function of the PMV window size.

In the following, we present two solution approaches for determining the lowest possible power consumption for a specific scenario.

3.1 Optimization-Based Solution

In the first approach, we evaluate the model based on a formulation of an optimization problem. For this purpose, we reformulate the bidirectional heat provided by the HVAC system as

$$\dot{Q}_{\text{hvac}} = \dot{Q}_{\text{hp}} - \dot{Q}_{\text{ac}}, \quad (21)$$

where $\dot{Q}_{\text{hp}} > 0$ represents the heat provided by the heating system and $\dot{Q}_{\text{ac}} > 0$ represents the heat removal by the AC system. Hence, the power demand of the HVAC system becomes

$$P_{\text{hvac}} = \frac{\dot{Q}_{\text{hp}}}{\gamma_{\text{hp}}(T_{\text{cab}} - T_{\infty})} + \frac{\dot{Q}_{\text{ac}}}{\gamma_{\text{ac}}(T_{\text{cab}} - T_{\infty})}, \quad (22)$$

where γ_{hp} and γ_{ac} represent the COP for heating and cooling, respectively. As opposed to eq. (15), this reformulation no longer relies on an absolute value and is therefore advantageous for derivative-based optimization algorithms. Additionally, the non-linear relationship in eq. (17), which is calculated in EN ISO 7730 in an iterative fashion, is approximated using a polynomial fit. Finally, we add a constraint to ensure that the RHs are operated according to their specified temperature $T_{\text{rh,tgt}}$:

$$T_{\text{rh}} = T_{\text{rh,tgt}}. \quad (23)$$

The optimization problem then reads as follows:

$$\begin{aligned} & \text{minimize } P_{\text{tot}}, \\ & \dot{Q}_{\text{hp}}, \dot{Q}_{\text{ac}}, P_{\text{rh}} \\ & \text{s.t. eqs. (16) and (20)–(23)}. \end{aligned} \quad (24)$$

Although in principle the reformulation introduced in eqs. (21) and (22) allows simultaneous heating and cooling, the optimal solution will not exhibit this suboptimal behavior.

Constraint eq. (23) corresponds to the RHs being always turned “on”. However, in typical summer conditions, using the RHs is obviously not useful. Instead of modeling this binary decision in our optimization, we formulate a second optimization problem, where the RHs are turned “off”, i.e., the corresponding equations are removed from the model. We then calculate the solutions to both optimization problems and select the solution with the lower overall power consumption P_{tot} . Hence, we assume that the RHs are only used if they reduce the overall power consumption. This solution procedure implemented in Matlab takes about 0.2s on a standard personal computer.

3.2 Alternative Approach

If the solution is to be computed without the use of an optimization algorithm, we suggest an alternative approach based on a root-finding problem. For this purpose, eqs. (16) and (23) can be completed with the following constraint for a fixed PMV target value Ψ_{tgt} :

$$\Psi = \Psi_{\text{tgt}}. \quad (25)$$

We thus arrive at a system of six equations, which can be solved for the six unknown variables T_{cab} , T_{rh} , $T_{\text{s,i}}$, $T_{\text{s,o}}$, \dot{Q}_{hvac} , and P_{rh} . Our approach therefore allows us to “invert causality” by prescribing a certain PMV and solving for the heat inputs. Equivalently, the system without RHs can be completed with eq. (25) and solved for the remaining four unknown variables. As in section 3.1, the solution with the lower overall power consumption P_{tot} is selected.

To find the solution minimizing the power consumption for an allowed PMV window, we first solve a reduced system with $\dot{Q}_{\text{hvac}} = 0$ and without eq. (25). If this solution violates eq. (20), we solve it again by setting the target PMV Ψ_{tgt} to the violated limit. Our implementation of this solution procedure takes about 0.3s on a standard personal computer. Simulation studies show that both solution algorithms presented yield the same results.

4. SCENARIOS

Our goal is to calculate the solution to not only a specific selection of environmental conditions, but to a large dataset of environmental conditions that are representative for a year-round operation of the city bus. Therefore, in this section, we first introduce the dataset that we use for these simulations. Second, we explain how passengers are placed in the bus cabin. Lastly, we propose an averaging scheme for the results on simulations of the entire dataset.

4.1 Data Sources

The number of passengers N_{pass} and the fraction of the door openings ζ_{door} are obtained from data recorded on a trolley bus in operation on various bus routes in Zürich. The mean ambient temperature T_{∞} , the DNI I_{dni} , and the DHI I_{dhi} are obtained from measurement data of MeteoSwiss. We average these time-resolved data values over operation periods of one hour to get scalar values for the corresponding variables. For convenience, fig. 3 shows an overview of the disturbances in all scenarios considered.

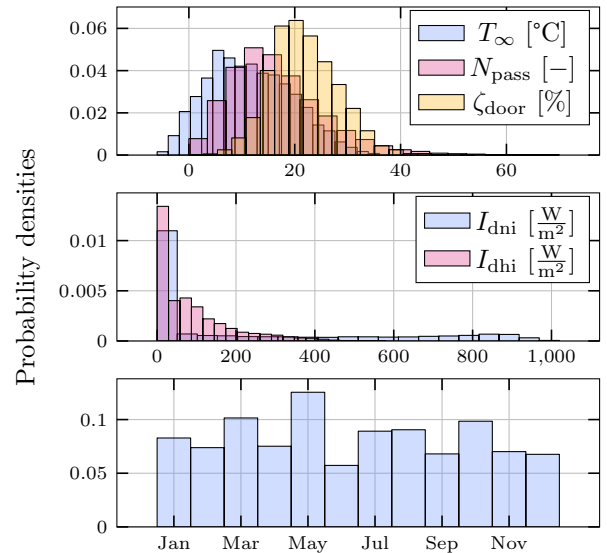


Fig. 3. Overview of the dataset of 7500 scenarios.

4.2 Passenger Placement

The placement of the passengers in the bus influences their thermal comfort due to their relative position to the RH surfaces. Since passenger positions are not recorded during operation, we adopt a pseudo-random placement strategy that ensures a realistic distribution throughout the cabin (see fig. 4 for a sample distribution).

4.3 Data Aggregation

As the scenarios recorded are not uniformly distributed throughout the year, as shown in fig. 3, we average the results over each month first, and then take the average of these values. In addition, since the perceived comfort is not monotone in the PMV scale (highest comfort at a value of zero), we cannot average the resulting PMV values from scenarios of various climatic conditions. For instance, the mean value of $\Psi = 1$ in summer and $\Psi = -1$ in winter is the same as the mean value of $\Psi = 0$ throughout the year, although the thermal comfort is of course better in the latter case. Therefore, we use the value for the predicted percentage dissatisfied (PPD), as suggested by EN ISO 7730. This quantity can be averaged over scenarios without the issues mentioned above.

5. RESULTS

In the following, we first present results for single scenarios for illustration purposes. Second, we show results that represent the year-round operation based on the averaging scheme introduced above.

5.1 Single-Scenario Results

Figure 4 shows the mean radiant temperature at $N_{\text{pass}} = 30$ different passenger locations, influenced by the RHs with a total surface area of $A_{\text{rh}} = 4\text{m}^2$ and a temperature $T_{\text{rh,tgt}} = 70\text{ }^\circ\text{C}$. The chosen RH layout achieves a more or less uniform mean radiant temperature for most passengers, except for those close to the front or rear of

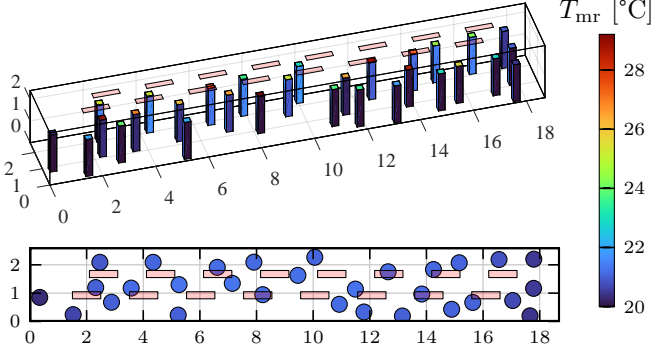


Fig. 4. Mean radiant temperatures perceived by passengers pseudo-randomly placed within the bus cabin (black outline) resulting from RH surfaces in the ceiling (light red). The isometric view on the top shows the mean radiant temperature of each surface, the top-view on the bottom shows each passenger’s area-averaged mean radiant temperature.

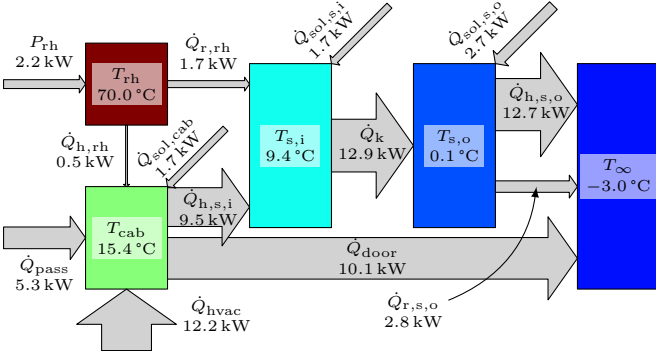


Fig. 5. Example heat flow overview for a cold winter scenario achieving “slightly cold” thermal comfort conditions, represented by $\Psi = -1$. The arrow annotations represent the corresponding absolute values.

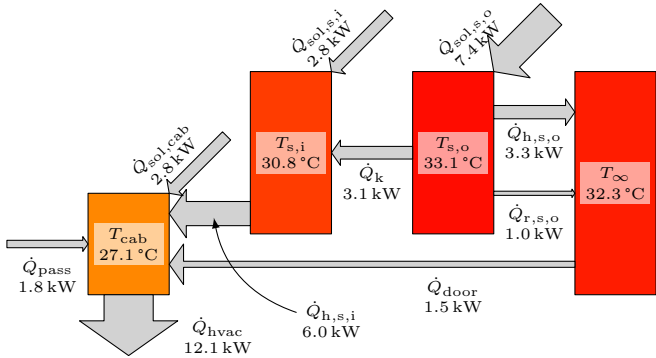


Fig. 6. Example heat flow overview for a hot summer scenario achieving “slightly warm” thermal comfort conditions, represented by $\Psi = 1$. The arrow annotations represent the corresponding absolute values.

the cabin, where the mean radiant temperature is close to the inside shell temperature of $T_{s,i} = 20^\circ\text{C}$.

Figures 5 and 6 visualize the optimal temperatures and power flows for a cold winter scenario and a hot summer scenario, respectively. For the winter scenario, the optimal cabin air temperature is fairly low, which can be explained,

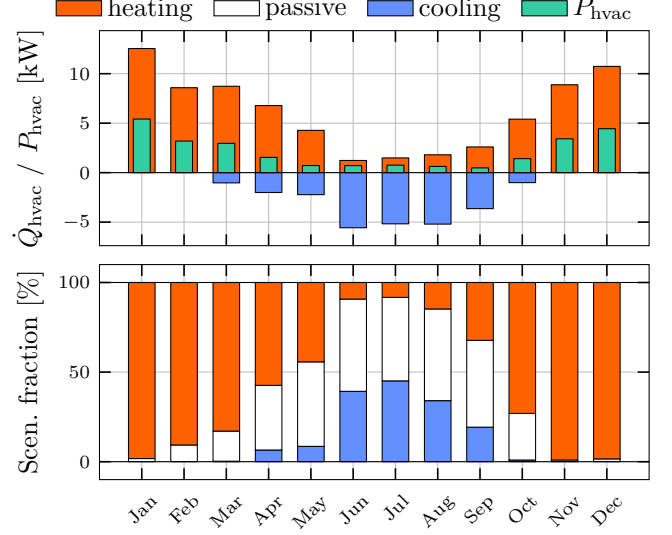


Fig. 7. Monthly averages of the heat \dot{Q}_{hvac} and the HVAC power consumption P_{hvac} required to achieve a PMV in the range $\Psi \in [-1, 1]$ on the top, and the fraction of the scenarios where heating or cooling is needed on the bottom.

on the one hand, by the high clothing insulation of $R_{\text{clo}} = 1.4$ clo, and, on the other hand, by the ability of the RHs to improve the thermal comfort through an increased mean radiant temperature. Still, the temperature difference to the ambient is substantial, which drives the significant thermal losses through the shell and the doors. In typical summer scenarios, we note that the solar irradiation can play a major factor. In the case shown here, it is even the main contributor. On the other hand, the conduction through the shell and the heat input through the doors typically is much less pronounced than in winter scenarios due to the smaller temperature difference between the cabin and the ambient.

5.2 Year-Round Performance

Monthly Averages: Figure 7 visualizes the monthly averages of the heat request \dot{Q}_{hvac} and the corresponding power consumption P_{hvac} . To simplify the interpretation of the results, no RHs are used in this case. The overview shows that the average heat demand is greater in winter than in summer, which is expected for the climate in central European. In addition, cooling is needed in much fewer instances than heating. In fact, for this case study, the overall heating demand (positive values of \dot{Q}_{hvac}) is about 8 times larger than the cooling demand. In cases where the comfort requirements can be achieved without heating or cooling, i.e., $\dot{Q}_{\text{hvac}} = 0$, the HVAC system is denoted “passive”.

Comparison of Heating Concepts: As heating is the more influential case, we investigate the performance of different heating concepts in this section. We compare a system with a purely electrical PTC heater with an efficiency of 100%, i.e., $\gamma_{\text{hp}} = 1$ to a system with an R407c HP with a COP γ_{hp} as shown in fig. 2. We refer to the two HVAC systems as “PTC-AC” or “HP-AC”, respectively. Both systems can be complemented with RHs. We do not change the cooling

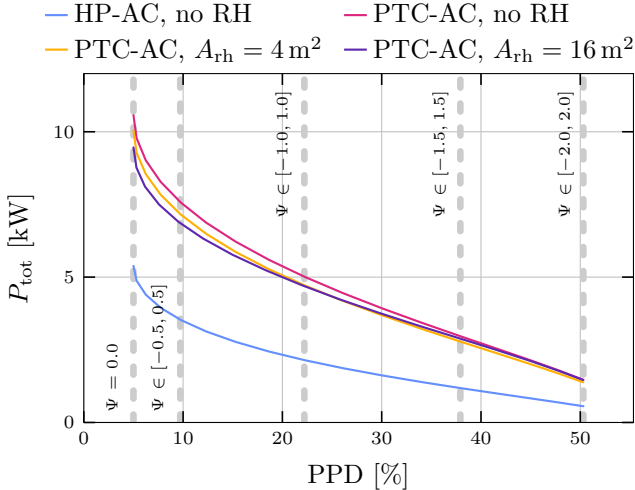


Fig. 8. Pareto front for different heating concepts showing the trade-off between the conflicting objectives of power demand and thermal discomfort.

system, i.e., we always use the R407c AC system with a COP γ_{ac} as shown in fig. 2.

The trade-off between the power consumption and the thermal comfort achieved by the different systems is visualized in fig. 8, where the allowed PMV is varied between $\Psi = 0$ (maximum comfort) and $\Psi \in [-2.0, 2.0]$ (least comfort). As explained in section 4.3, we use the predicted percentage dissatisfied (PPD) value for data averaging. As expected from the definition of the PPD in EN ISO 7730, a value below 5% can never be reached in practice. The power demand increases more rapidly the lower the PPD.

Figure 8 shows that RHs can reduce the mean HVAC power consumption of the PTC-AC system by 5% to 10% depending on the comfort requirements. Our analyses show that greater values of T_{rh} generally improve the performance of the RHs due to the fourth power-dependency in radiation compared to convection. Therefore, we use a very high $T_{rh,tgt} = 90^\circ\text{C}$ for deriving fig. 8. Furthermore, fig. 8 shows that increasing the RH panel size is beneficial for high comfort requirements. Although we are aware that an implementation with very large heater surfaces and high temperatures in reality is questionable, the configuration serves as a best-case estimate of the achievable energetic benefit.

Comparing the PTC-AC heating system with a HP-AC system, fig. 8 shows that the latter can reduce the consumption by 50% to 60%. An extensive search for RH configurations (size and temperature) to complement the HP reveals that the reduction in power consumption is limited to around 0.3%. Considering the added complexity of RH installation and the investment costs, thus conclude that RHs are not a reasonable addition to a HP. This observation is also confirmed in simulations with lower and higher ambient annual mean temperatures.

Sensitivity Study: Finally, we show the results of a sensitivity study in fig. 9. Similar to what is shown in fig. 7, this study is also conducted on a HP-AC system without RHs. The metabolic heat rate \dot{Q}_{met} has the highest relative influence on the mean power consumption.

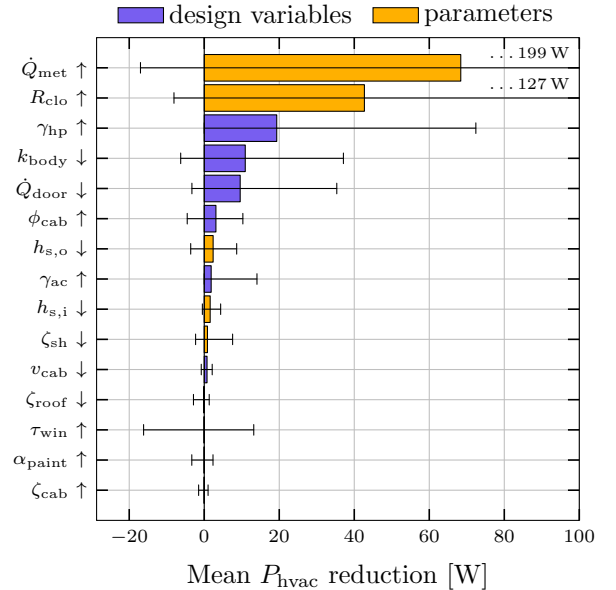


Fig. 9. Sensitivity of the annual mean power consumption with respect to 1% changes in model parameter values. Each parameter is marked with \uparrow or \downarrow to indicate if its value is increased or decreased by 1%, respectively. To increase clarity, parameters that can be influenced in the vehicle design process are marked as “design variables”. The whiskers show the 5th and 95th percentiles of all scenarios, respectively. As two of them exceed the graph, they are represented by numerical values.

It influences the model in two ways: First, as a heat input in eq. (1), and second, in the calculation of the PMV. Unsurprisingly, the clothing insulation factor R_{clo} also has a strong influence on the mean power consumption. In terms of design variables, the largest leverage is expected by an increase in γ_{hp} . On the other hand, an increase in γ_{ac} does not provide a benefit nearly as large, as expected due to the lower cooling requirements shown in fig. 7. This observation further encourages the use of alternative refrigerants, such as CO_2 (R744), which offer advantages in heating efficiency, even if they come at a disadvantage in cooling efficiency.

Increasing the insulation, (i.e., decreasing the thermal conductance k_{body}) or decreasing the door losses, e.g., by using air curtains, can improve the energy efficiency in a similar manner. For most of the parameters affecting the solar heat input, such as the window transmissivity τ_{win} , the positive and negative effects roughly cancel each other out.

6. CONCLUSION

6.1 Contributions

In this paper, we propose mathematical models of HVAC systems of an electric city bus, which can be used to efficiently derive the Pareto front between power consumption and comfort requirements subject to a set of scenarios that represent a year-round operation. Therefore, we propose a steady-state formulation, for which two alternative solution approaches are presented. The results show that

HP-AC system can lower the overall annual HVAC power consumption by 50% to 60% compared to a PTC-AC system, without affecting thermal comfort. Alternatively, RHs can be used as a complement to PTC heaters to reduce the power consumption by up to 10%. However, no significant benefit is found from complementing a HP with RHs. Finally, a sensitivity study motivates the further promotion of CO₂ HPs, due to their potentially higher heating COP. Further efficiency benefits can be expected by improvements in insulation and a reduction of door losses, while material properties related to solar irradiation, such as absorptivity or transmissivity, seem to have only a negligible influence.

6.2 Outlook

For further research, we propose three distinct directions.

First, the models used in this work could be refined. The most restricting assumptions in our opinion are the uniform temperatures of the shell and the air and the greatly simplified cabin and passenger geometry (no interior, no sitting passengers, no driver compartment, no shading from infrared heat). Additionally, the thermal comfort model could be refined to consider temperature asymmetry (particularly in the presence of RHs) and more realistic relative humidity values.

Second, using the proposed model for component size optimization is a promising idea. For this purpose, the model needs to be extended to consider component limitations such as the maximum heating capacity on the one hand and the component weights on the other. In this case, the traction performance should also be included.

Third, the current formulation averages the PPD over all scenarios, although the number of passengers varies greatly. It might be an interesting extension to use the number of passengers for a weighted PPD average both for the evaluation and for the allocation of HVAC power. In this way, it might be beneficial to select a narrow PMV window in scenarios with many passengers. Such a consideration requires a connection of all scenarios into a single optimization problem.

REFERENCES

- Bibra, E.M., Connelly, E., Dhir, S., Drtil, M., Henriot, P., Hwang, I., Marois, J.B.L., McBain, S., Paoli, L., and Teter, J. (2022). Global EV outlook. Technical report, International Energy Agency – IEA, Paris, France. URL <https://www.iea.org/reports/global-ev-outlook-2022>.
- Centeno Brito, M., Santos, T., Moura, F., Pera, D., and Rocha, J. (2021). Urban solar potential for vehicle integrated photovoltaics. *Transportation Research Part D: Transport and Environment*, 94, 102810. doi:10.1016/j.trd.2021.102810.
- Cigarini, F., Fay, T.A., Artemenko, N., and Göhlich, D. (2021). Modeling and experimental investigation of thermal comfort and energy consumption in a battery electric bus. *World Electric Vehicle Journal*, 12(1). doi:10.3390/wevj12010007.
- Cvok, I., Ratković, I., and Deur, J. (2021). Multi-objective optimisation-based design of an electric vehicle cabin heating control system for improved thermal comfort and driving range. *Energies*, 14(4). doi:10.3390/en14041203.
- EN ISO 6946 (2017). Building components and building elements – thermal resistance and thermal transmittance – calculation methods. Norm, European Committee for Standardization, Brussels, Belgium.
- EN ISO 7730 (2005). Ergonomics of the thermal environment – analytical determination and interpretation of thermal comfort using calculation of the PMV and PPD indices and local thermal comfort criteria. Norm, European Committee for Standardization, Brussels, Belgium.
- Fanger, P.O. (1970). *Thermal Comfort: Analysis and Applications in Environmental Engineering*. Danish Technical Press, Copenhagen, Denmark.
- Gross, U., Spindler, K., and Hahne, E. (1981). Shapefactor-equations for radiation heat transfer between plane rectangular surfaces of arbitrary position and size with parallel boundaries. *Letters in Heat and Mass Transfer*, 8(3), 219–227. doi:10.1016/0094-4548(81)90016-3.
- Hanke, D. (2018). Das Ei des Kolumbus? EBus-Cluster Concept optimiert Nebenverbraucher. *Omnibus Spiegel*, 40(10), 10–12.
- Havenith, G., Fiala, D., Błażejczyk, K., Richards, M., Bröde, P., Holmér, I., Rintamaki, H., Benschabat, Y., and Jendritzky, G. (2012). The UTCI-clothing model. *International Journal of Biometeorology*, 56, 461–470. doi:10.1007/s00484-011-0451-4.
- Incropera, F.P., DeWitt, D.P., Bergmann, T.L., and Lavine, A.S. (2007). *Fundamentals of Heat and Mass Transfer*. John Wiley & Sons, Hoboken, NJ, 6 edition.
- Qi, Z. (2014). Advances on air conditioning and heat pump system in electric vehicles – a review. *Renewable and Sustainable Energy Reviews*, 38, 754–764. doi:10.1016/j.rser.2014.07.038.
- Ramsey, D., Bouscayrol, A., Boulon, L., Desreuveaux, A., and Vaudrey, A. (2022). Flexible simulation of an electric vehicle to estimate the impact of thermal comfort on the energy consumption. *IEEE Transactions on Transportation Electrification*, 8(2), 2288–2298. doi:10.1109/TTE.2022.3144526.
- Schaut, S. and Sawodny, O. (2020). Thermal management for the cabin of a battery electric vehicle considering passengers’ comfort. *IEEE Transactions on Control Systems Technology*, 28(4), 1476–1492. doi:10.1109/TCST.2019.2914888.
- Schälin, A. (1998). Gebäudeeingänge mit grossem Publikumsverkehr. Technical report, AFC Air Flow Consulting, Weinbergstr. 72, 8006 Zürich. Appendix A.
- Sidler, F., Ineichen, S., and Zweifel, G. (2019). Messung Energieverlust durch Türöffnungen bei Linien-Bussen. Schlussbericht 098 (des ESöV 2050-Programms), Bundesamt für Verkehr BAV. URL <https://www.aramis.admin.ch/Grunddaten/?ProjectID=43762>.